Journal of Materials Chemistry A

Electronic Supplementary Information

Highly efficient electrochemical and chemical hydrogenation of 4-nitrophenol using recyclable narrow mesoporous magnetic CoPt nanowires

Albert Serrà,[a] Xavier Alcobé, [b] Jordi Sort, [c, d] Josep Nogués[d, e] and Elisa Vallés[a, *]

[a.] *Grup d'Electrodeposició de Capes Primes i Nanoestructures (GE-CPN), Departament de Ciència de Materials i Química Física and Institut de Nanociència i Nanotecnologia (IN²UB), Universitat de Barcelona, Martí i Franquès, 1, E-08028, Barcelona, Catalonia, Spain.*

[b.] *Unitat de DRX, Centres Científics i Tecnològics, Universitat de Barcelona, CCiTUB, Lluís Solé i Sabarís, 1–3, E-08028, Barcelona, Catalonia, Spain.*

[c.] *Departament de Física, Universitat Autònoma de Barcelona, E-08193, Bellaterra, Catalonia, Spain.*

[d.] *ICREA, Pg. Lluís Companys 23, 08010, Barcelona, Spain.*

[e.] *Catalan Institute of Nanoscience and Nanotechnology (ICN2), CSIC, The Barcelona Institute of Science and Technology, Campus UAB, E-08193, Bellaterra, Catalonia, Spain.*

Cronoamperometric curves of the nanowires electrosynthesis

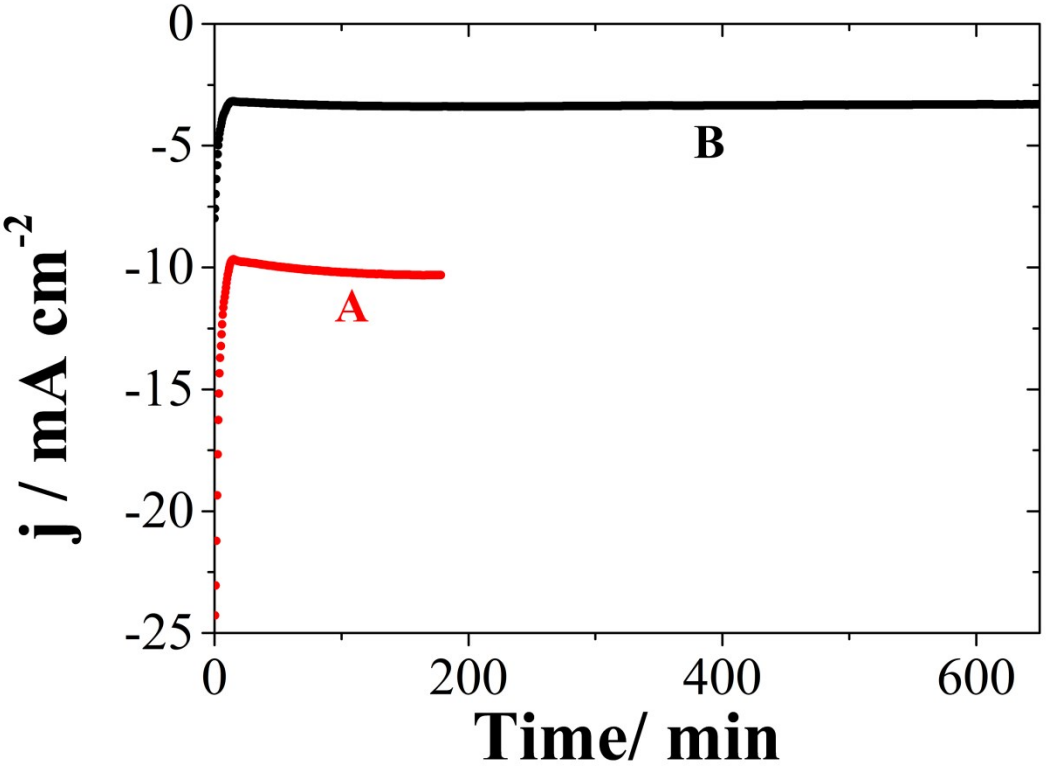

Figure 1S: Cronoamperometric curves of the electrosynthesis inside the nano-channels of alumina membranes, at -1.0 V vs Ag/AgCl and 25 ºC, of Co–Pt nanowires to attain the same deposition charge density (2.1 C cm^{-2}) in (A) aqueous solution and (B) IL/W microemulsion.

FE-SEM images of alumina membranes

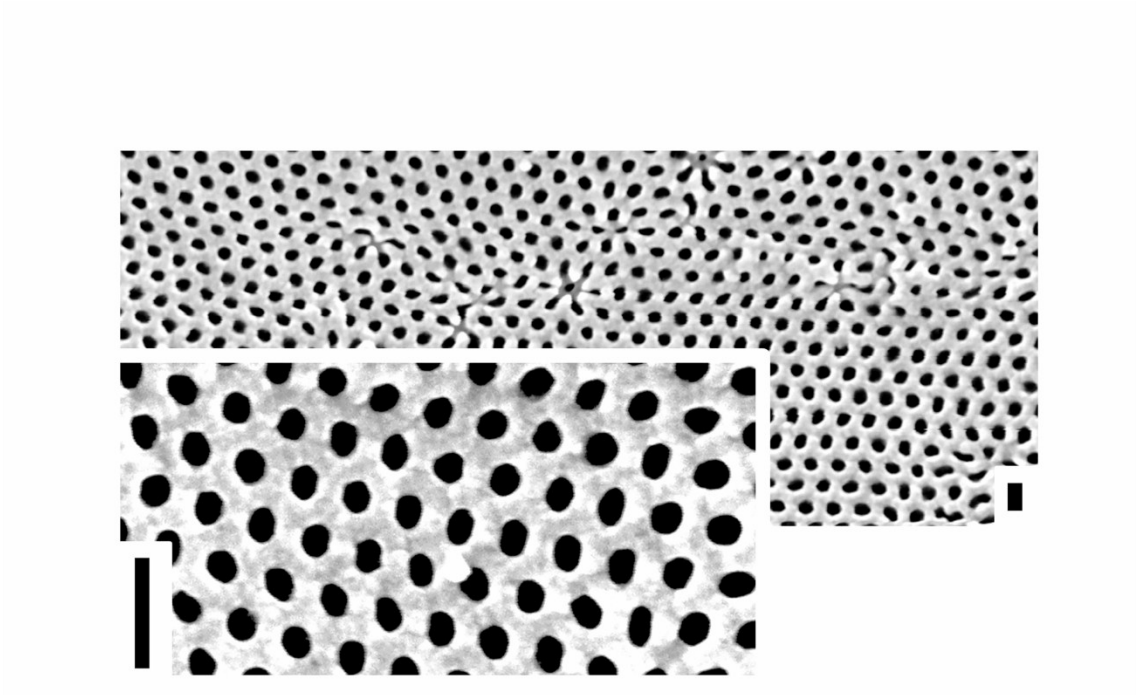

Figure 2S: FE-SEM micrographs of alumina membranes used to synthesize nanowires. Scale bar: 100 nm.

TEM-Energy dispersive X-ray spectroscopy and HR-TEM

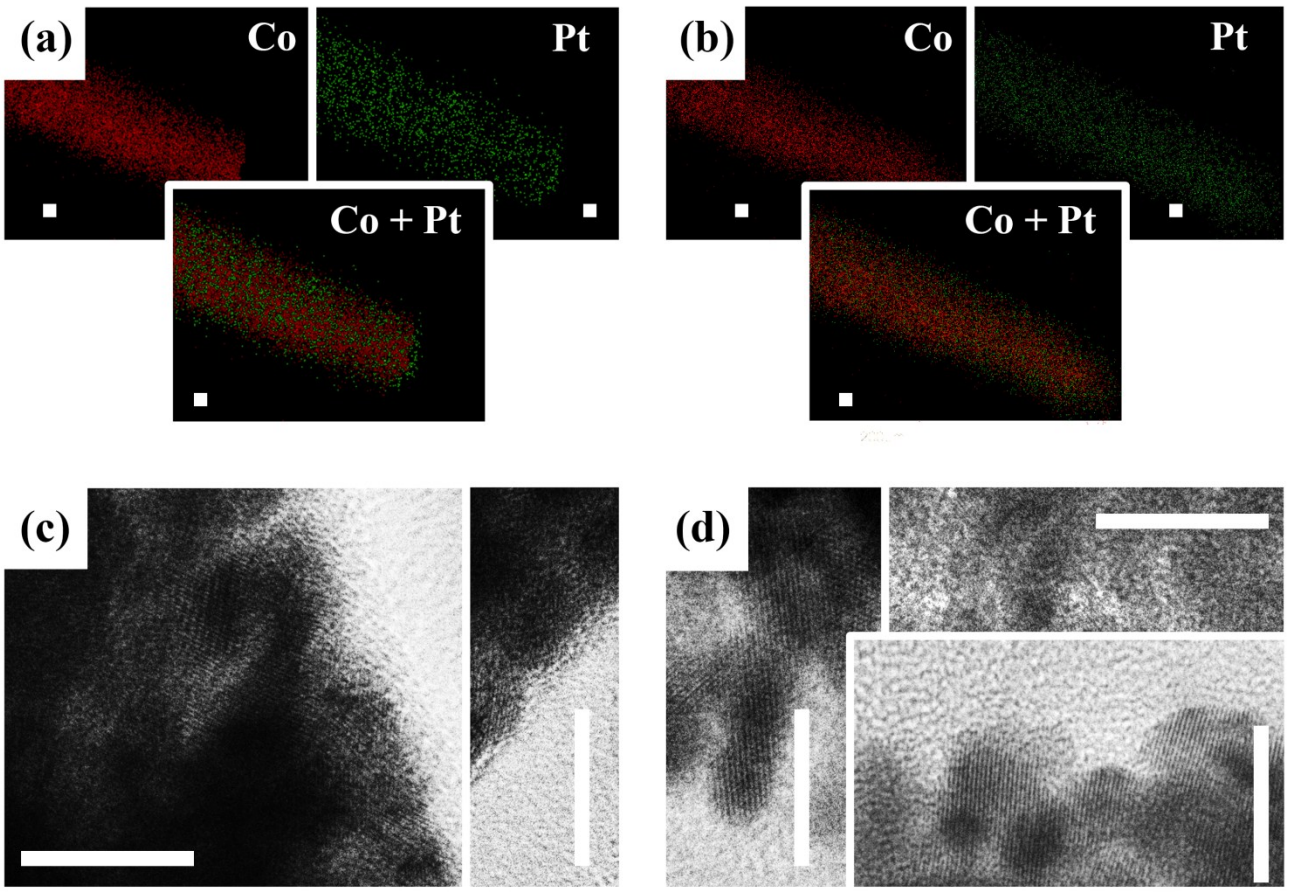

Figure 3S: Elemental mapping of Co–Pt compact (a) and mesoporous (b) NWs using an EDS-TEM and HRTEM images of compact (c) and mesoporous (d) NWs. Scale bar: 5 nm.

X-Ray Diffraction characterization

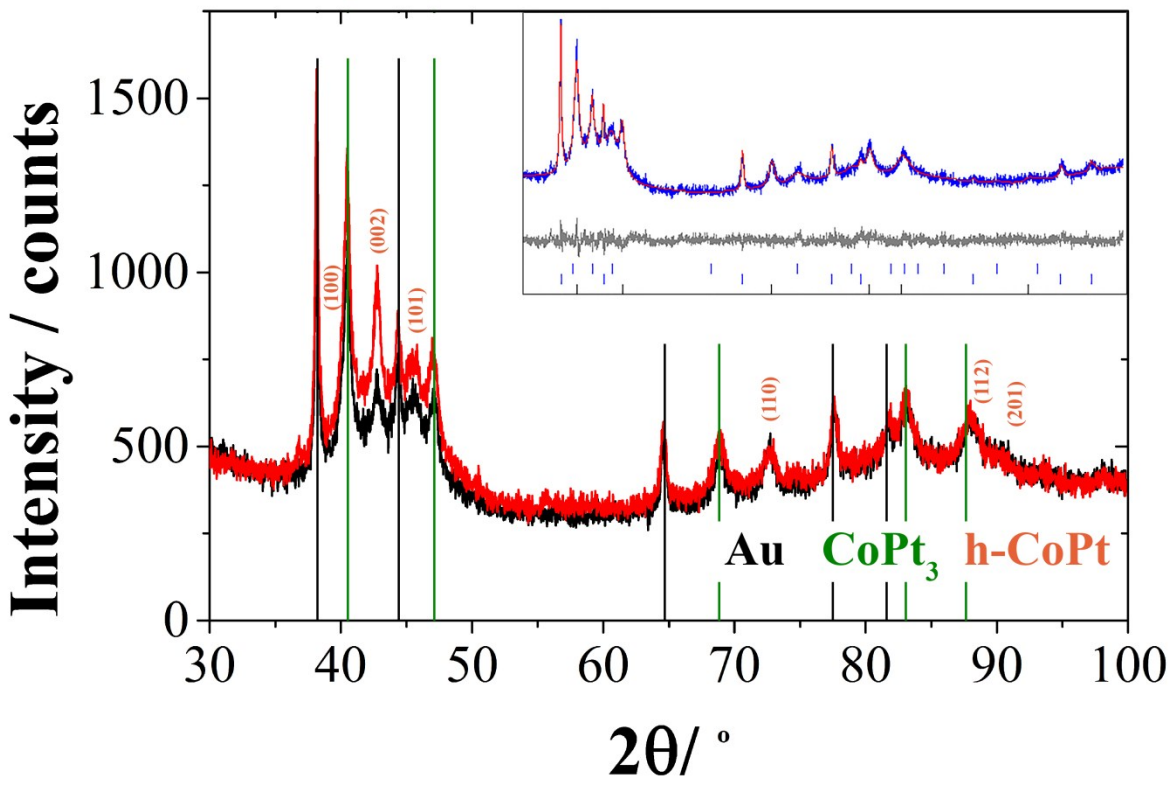

Figure 4S: XRD patterns of the two NW's samples: compact (red) and mesoporous (black). The position of the main Au and $CoPt_3$ are indicated by vertical bars, while the miller indexes of the main peaks of the hexagonal CoPt (h-CoPt) phase are indicated next to the corresponding peaks. Inset: Experimental (blue) and Rietveld fit (red) XRD patterns of the compact nanowires. The residuals of the fit are shown in grey at the bottom of the graph.

From the x-ray diffraction (XRD) patterns two phases were immediatelly identified: *fcc* Au, corresponding to some remaining gold in the nanowires, and *fcc* $CoPt_3$ (Pm-3m) (see Figure 3S). The remaining peaks are indexed to a hexagonal *hcp* phase, assigned to a CoPt alloy (i.e., the same phase as *hcp* Co but very distorted due to the incorporation of Pt atoms in the crystalline lattice – $P6_3mmc$). Rietveld profile analyses were performed using the TOPAS v5 software. [1,3] Note that the Co–Pt phase was treaded and refined by profile pattern mathcing according to Pawley. [4]

The parameters obtained from the fit are summarized in **Table 1S.**

NW type	Phase	Cell parameters / Å		Crystallite size / nm
Compact	$CoPt_3$ *fcc*	a = 3.855		11.9
	CoPt *hcp*	a = 2.603	c = 4.222	4.8
Mesoporus	$CoPt_3$ *fcc*	a = 3.855		11.4
	CoPt *hcp*	a = 2.604	c = 4.211	5.4

Table 1S. Cell parameters and crystallite size of $CoPt_3$ and CoPt phases in the compact and mesoporous NWs.

Magnetic Properties

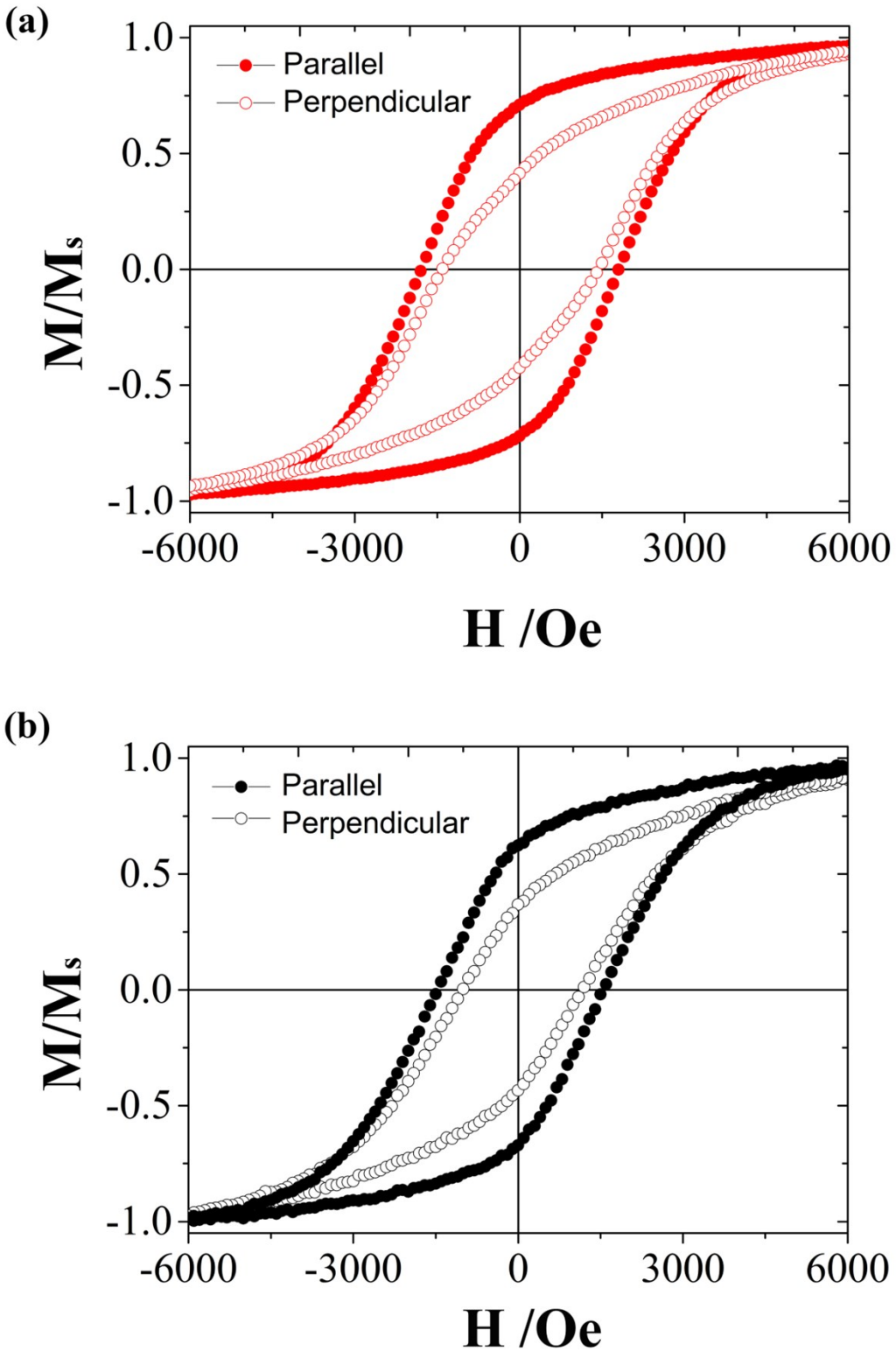

Figure 5S: Room-temperature (300 K) parallel and perpendicular to the wire axis hysteresis loop of the compact (a) and mesoporous (b) Co–Pt NWs.

Electrochemical Surface Areas (ECSAs) of Co–Pt NWs

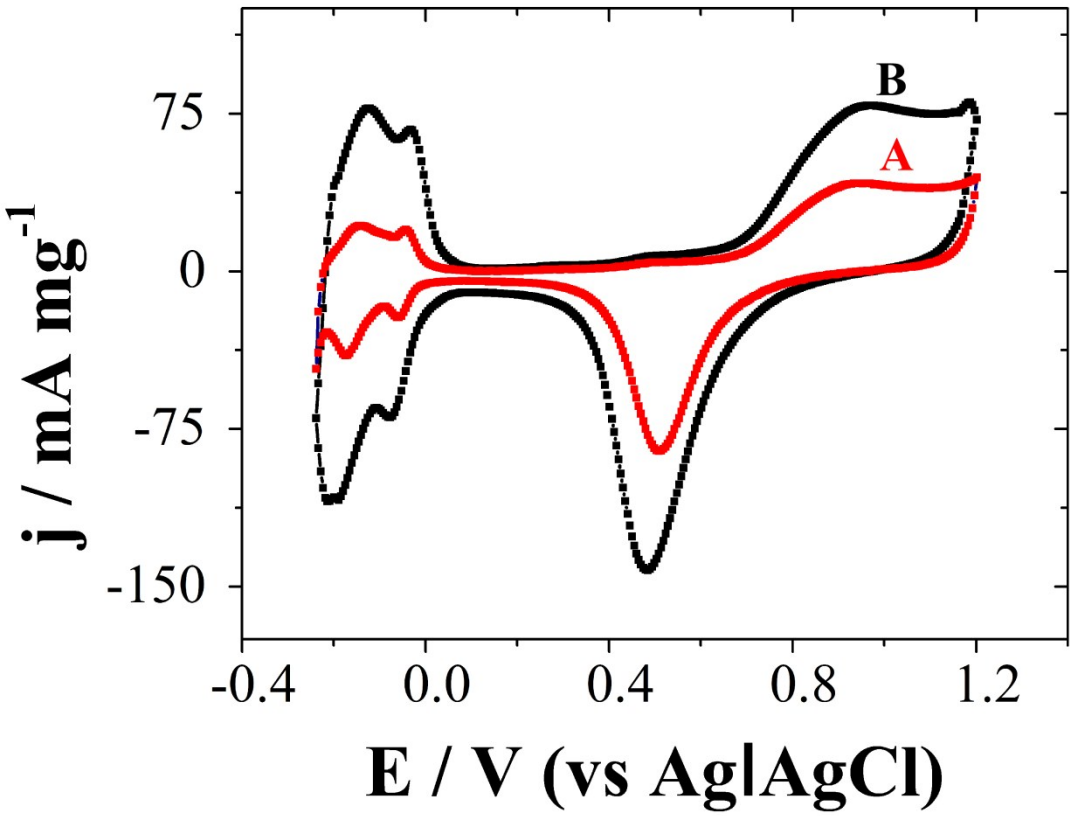

Figure 6S: Cyclic voltammetry in H_2SO_4 0.5 M solutions at 25 ºC with a scan rate of 20 mV s^{-1} for Co-Pt compact (A) and mesoporous (B) NWs.

UV–visible spectra of 4-nitrophenol and 4-aminophenol

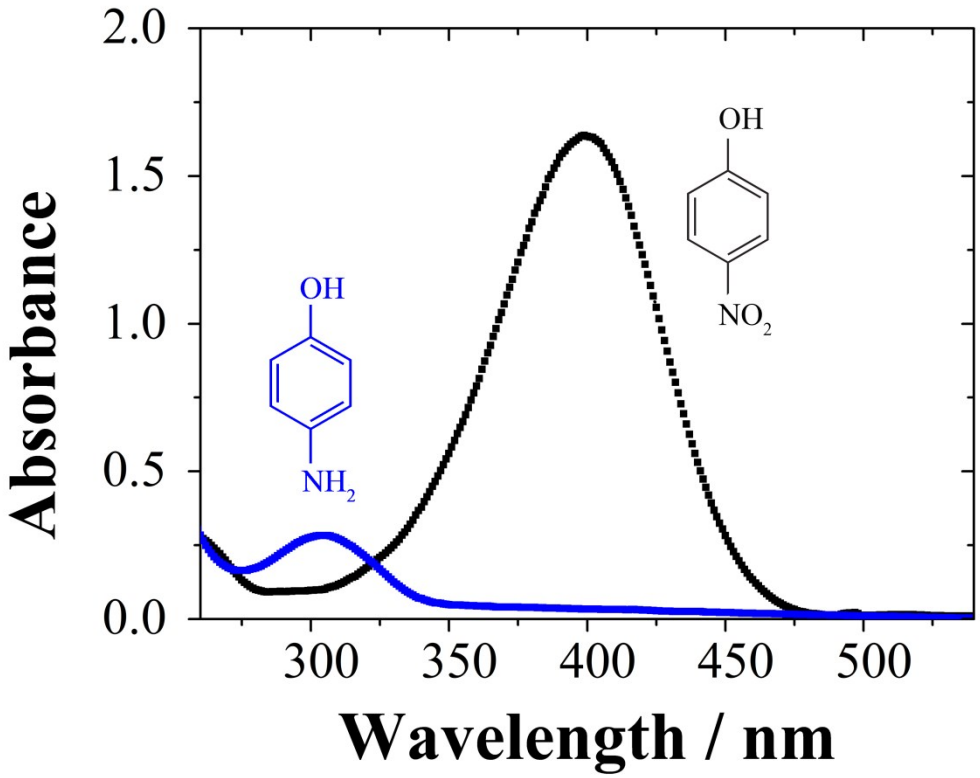

Figure 7S: UV–visible spectra of 4-nitrophenol and 4-aminophenol.

Comparison of the catalytic performance

Catalyst	K_{app} / ms^{-1}	K_{nor} / s^{-1} g^{-1}	Reference
Compact Co – Pt NWs	1.8	1538	This work
Mesoporous Co – Pt NWs	5.7	4713	This work
PCN-224-700	5.3	-	5
Pt–Au pNDs/RGOs	3.8	926	6
Pd micromotor	6.6	-	7
Pt3Au1-PDA/RGO	9.6	1700	8
Pt55Pd38Bi7 nanowires	5.2	74	9
MSNCs–Ag	17.0	850	10
AuPd nanocrystals	5.2	74	11
Fe@Au-ATPGO	1.4	400	12

Table 2S: Comparison of the catalytic performances of Co–Pt NWs with other catalysts previously reported for the reduction of 4-NP.

Electrochemical Surface Area after be used as electro-catalysts

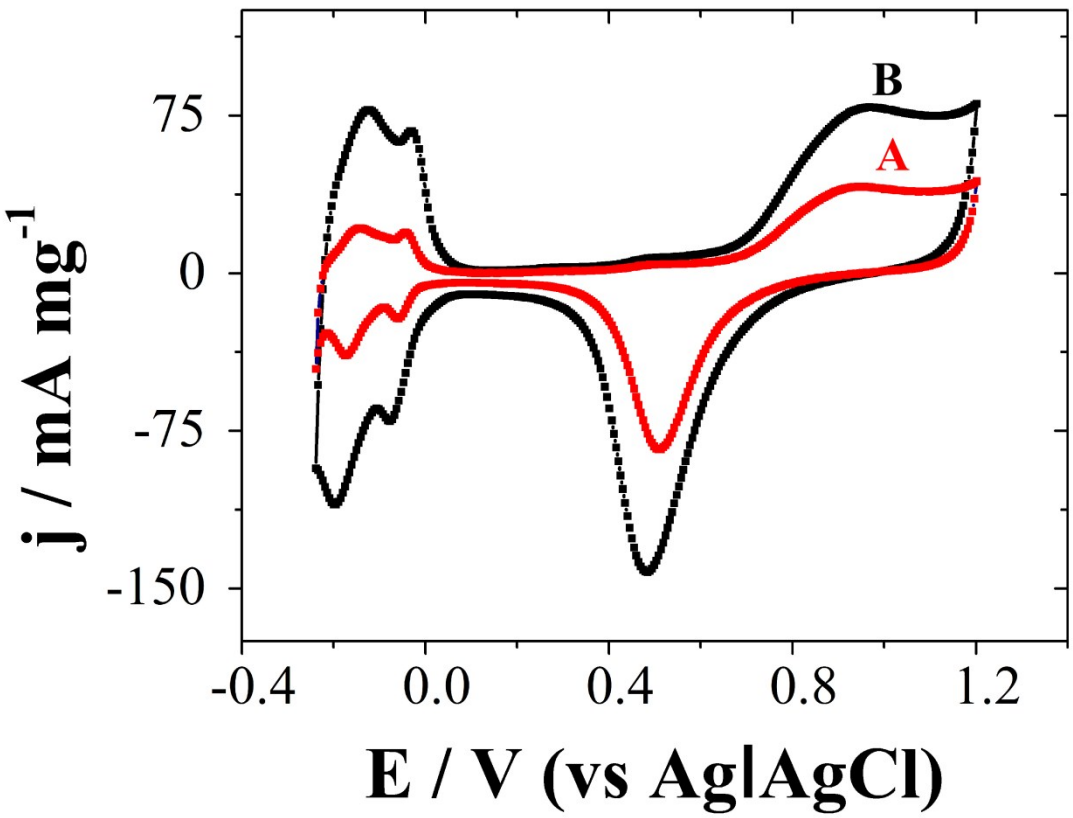

Figure 8S: Cyclic voltammetry in H_2SO_4 0.5 M solutions at 25 ºC with a scan rate of 20 mV s^{-1} for Co-Pt compact (A) and mesoporous (B) NWs after be used as electro-catalysts.

Time-dependent UV–Visible spectra of 4-NP catalysed reduction – Pure Pt and Co NWs

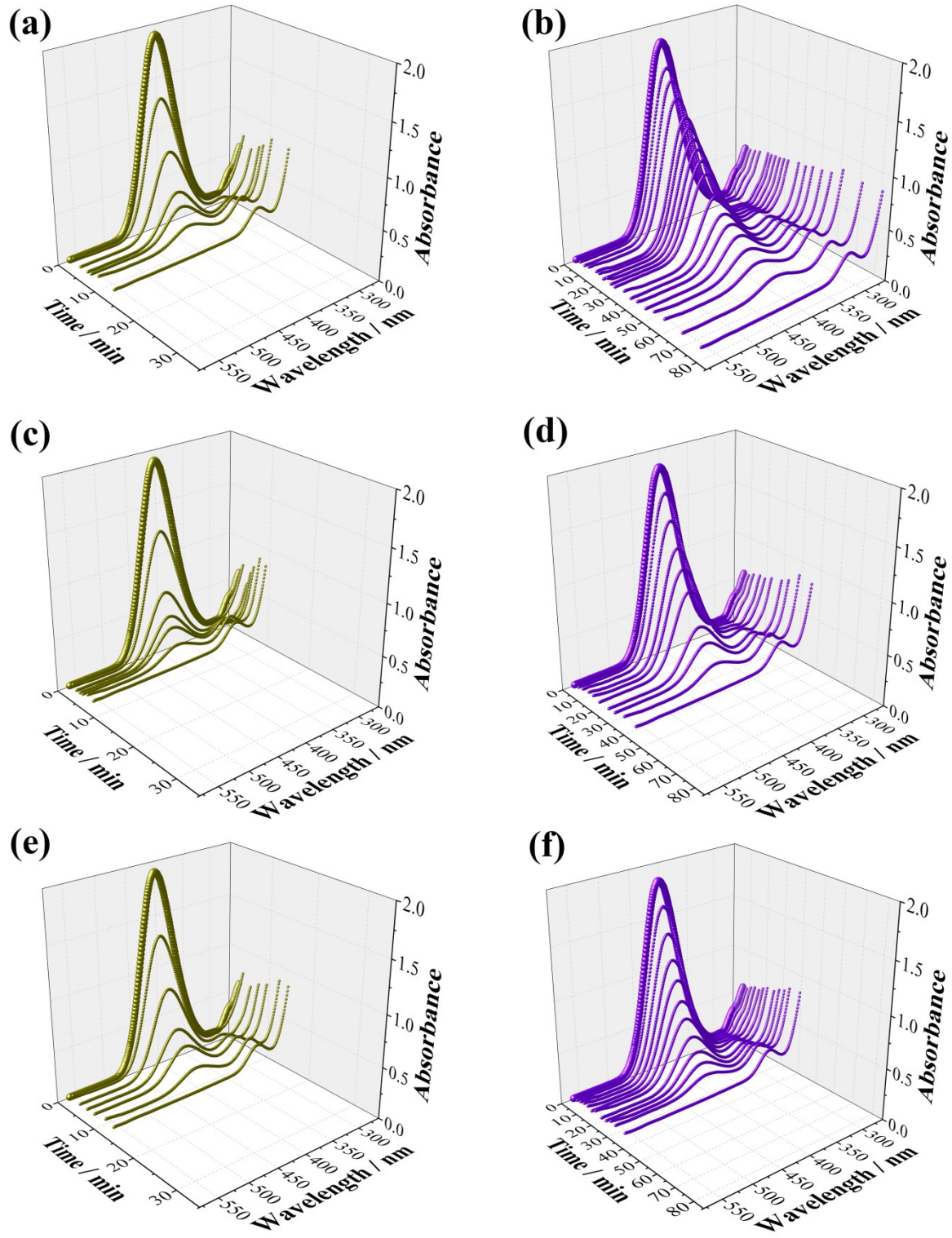

Figure 9S: Time-dependent UV–Visible spectra of 4-NP catalysed reduction in silent (panels a and b, for pure Pt and Co mesoporous NWs, respectively), intermittent ultrasound stirring (panels c and d, for pure Pt and Co mesoporous NWs, respectively) and magnetic stirring (panels e and f, for pure Pt and Co mesoporous NWs, respectively) conditions, in which 12 µL of a suspension of catalyst (0.1 mg mL^{-1}) were added.

Kinetic constants – Pure Pt and Co NWs

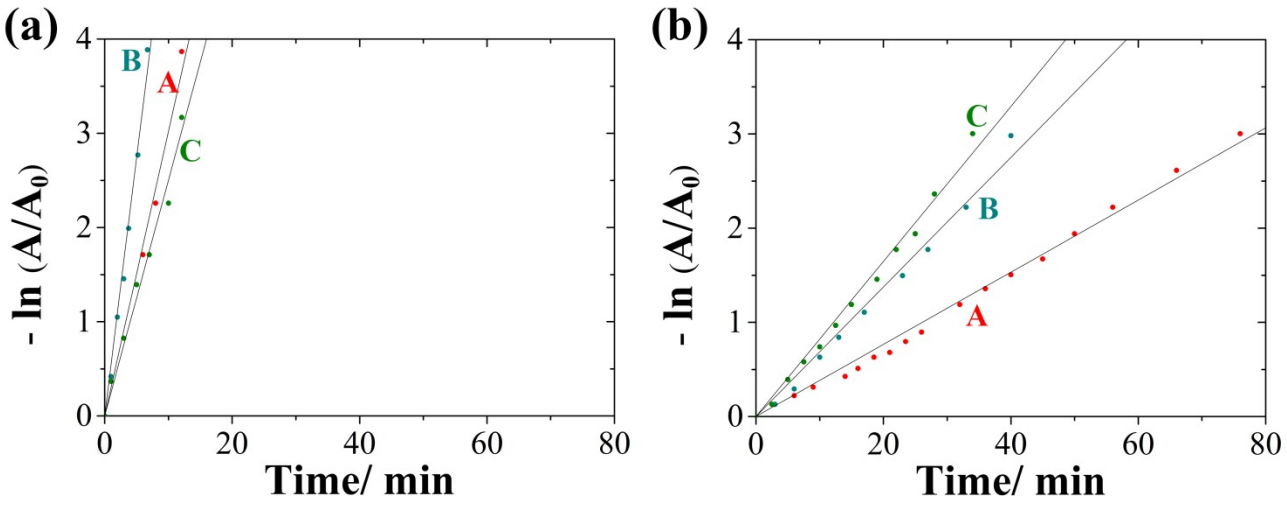

Figure 10S: Plots of $-ln(A/A_0)$ against reaction time for the catalysed reduction of 4-NP by (a) Pt and (b) Co mesoporous NWs in silent (A), intermittent ultrasound stirring (B) and magnetic stirring (C) conditions.

Catalyst Reusability

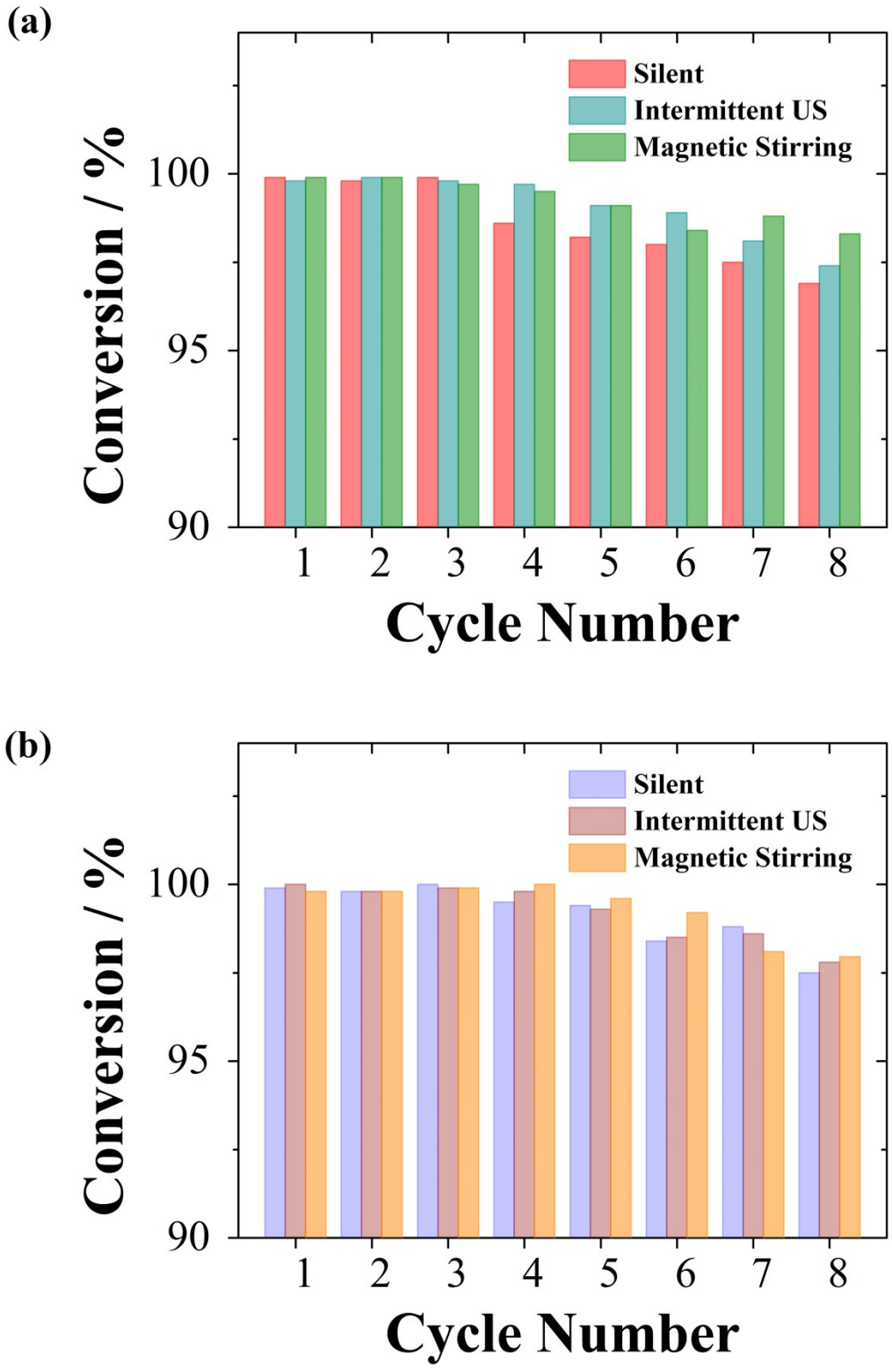

Figure 11S: Reusability of Co–Pt compact (a) and mesoporous (b) NWs as the catalyst for the reduction of 4-NP in eight successive cycles.

References

[1] H. Rietveld, *J. Appl. Cryst.,* 1969, ***2***, 65.
[2] A. Coelho, J. Evans, I. Evans, A. Kern, and S. Parsons, *Powder Diffr*. 2011, **26**, S22.
[3] Bruker AXS. (2011). TOPAS, v5.0 (Computer Software). *Bruker AXS*. Karslruhe, Germany.
[4] G. S. Pawley, *J. Appl. Cryst.* 1981, **14**, 357.
[5] G. Huang, L. Yang, X. Ma, J. Jiang, S.-H. Yu, and H.-L. Jiang, *Chem. Eur. J.* 2016, **22**, 3470.
[6] J.-J. Lv, A.-J. Wang, X. Ma, R.-Y. Xiang, J.-R. Chen, and J.-J. Feng, *J. Mater. Chem. A* 2015, **3**, 290.
[7] S. K. Srivastava, M. Guix, and O. G. Schmidt, *Nano Lett.* 2016, **16**, 817.
[8] W. Ye, J. Yu, Y. Zhou, D. Gao, D. Wang, C. Wang, and D. Xue, *Appl. Catal. B-Environ.* 2016, **181**, 371.
[9] Y.-Y. Shen, Y. Sun, L.-N. Zhou, Y.-J. Li, and E. S. Yeung, *J. Matter. Chem. A* 2014, **2**, 2977.
[10] G. Cui, Z. Sun, H. Li, Z. Liu, Y. Tian, and S. Yan, *J. Mater. Chem. A* 2016, **4**, 1771.
[11] S. K. Ghosh, M. Mandal, S. Kundu, S. Nath, and T. Pal, *Appl. Catal. A*, 2004, **268**, 61.
[12] V. K. Gupta, N. Atar, M. L. Yola, Z. Üstündag, and L. Uzun, *Water Res.* 2014, **48**, 210.

